Exploring the Intracluster Magnetic Fields through Radio and X-ray Observations

M. Takizawa, I. Takahashi (Yamagata Univ.),
T. Ozawa, H. Nakanishi, T. Akahori (Kagoshima Univ.)
and others

JVLA S- and X-band polarimetry of the merging cluster Abell 2256
Ozawa et al. (2015) PASJ, 67, 110

Hot spots in the XMM sky:
Cosmology from X-ray to Radio
Mykonos Island, 17 June 2016

Observational Evidence of Intracluster Magnetic Field (1): Radio Halos / Relics

Non-thermal radio emission from merging clusters of galaxies

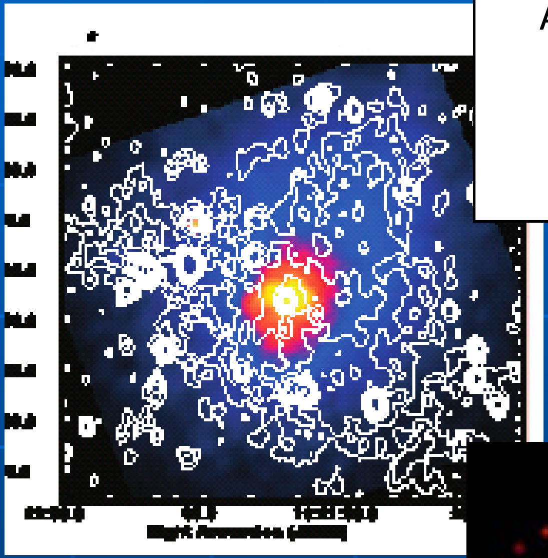

Abell 2319 with Radio Halo
Rosat X-ray image (colors)
Radio image (contours)
Feretti et al. (1997)

synchrotron radio

$\gamma \sim 10^4$ electrons + 0.1-10μG B

Hard X-ray will be emitted through Inverse compton with CMB

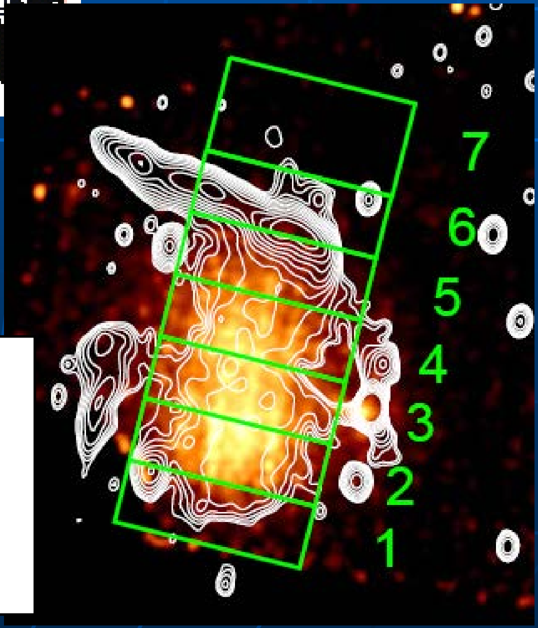

1RXS J0603.3+4214 with “Toothbrush”Radio Relic
Suzaku X-ray image (colors)
Radio image (contours)
Itahana et al. (2015), Evening Session Today

Observational Evidence of Intracluster Magnetic Field (2): Faraday Rotation

- Polarized plains of linear polarized radio wave rotate when propagating through the magnetized plasma.

$$\Delta\theta = \frac{2\pi e^3}{m^2 c^2 \omega^2} \int_0^d n B_{\parallel} \, ds.$$

- Polarized radio sources observations in and behind clusters suggest random magnetic field structures.

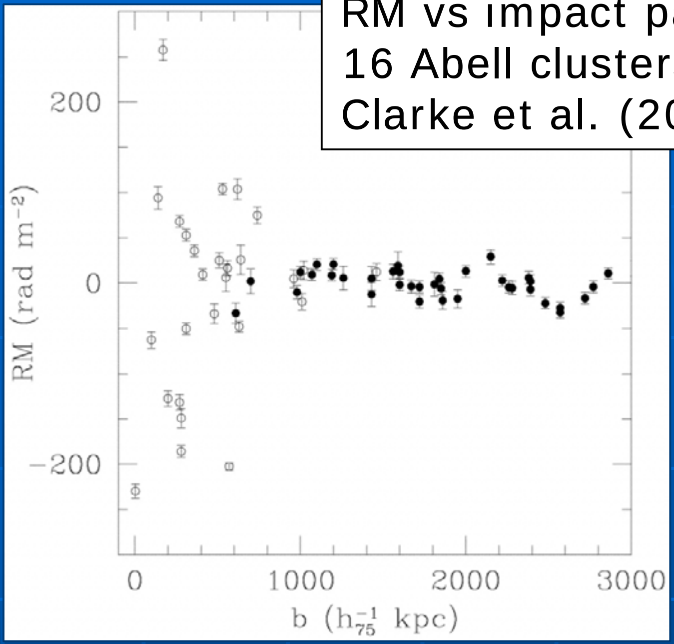

RM vs impact paameter for 16 Abell clusters
Clarke et al. (2001)

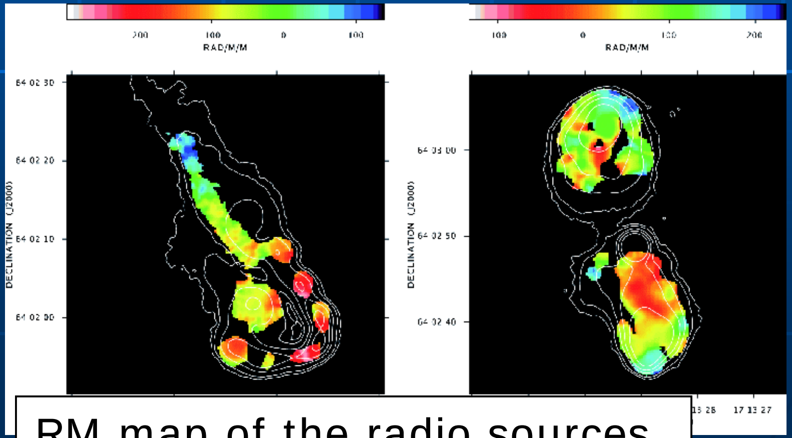

RM map of the radio sources in Abell 2255
Govoni et al. (2006)

Depolarization because of random magnetic fields

External Faraday Dispersion

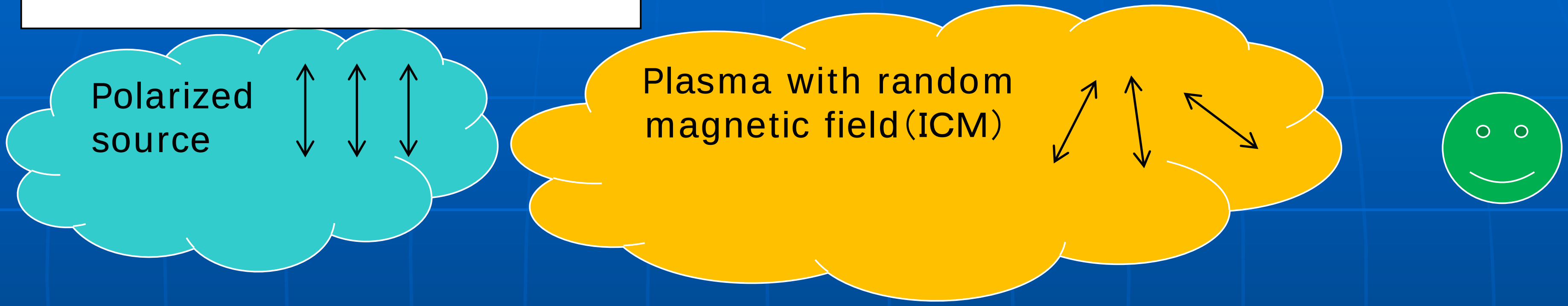

- Because of frequency dependence of FR($\Delta\theta \propto \omega^{-2}$), depolarization is more prominent in lower frequency (or longer wavelength).

$$p_{\mathrm{EFD}} = p_0 e^{-S}$$

$$S = 2\sigma_{\mathrm{RM}}^2 \lambda^4$$

Burn's law (Burn 1966)
p_{EFD}: observed fractional polarization
p_0: intrinsic fractional polarization
σ_{RM}: standard deviation of RM

Abell 2256

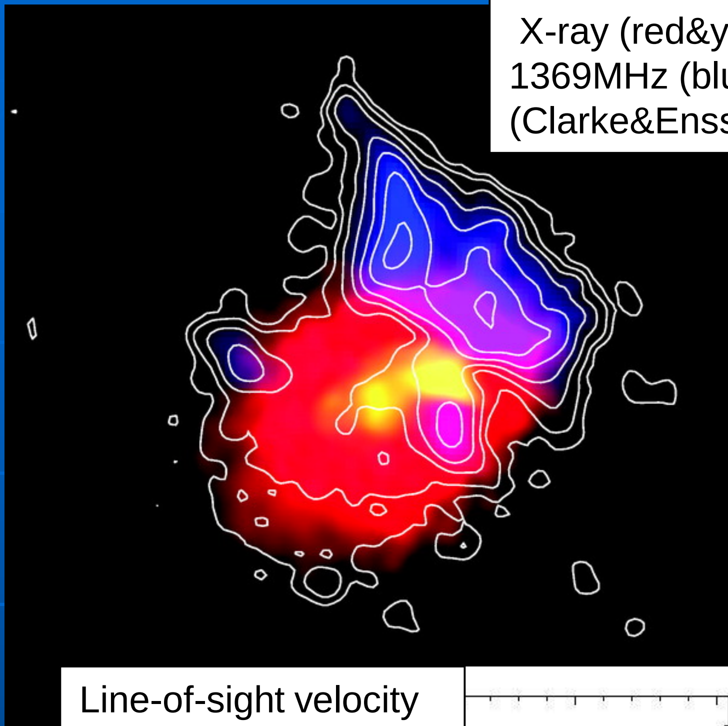

X-ray (red&yellow)
1369MHz (blue&contours)
(Clarke&Ensslin 2006)

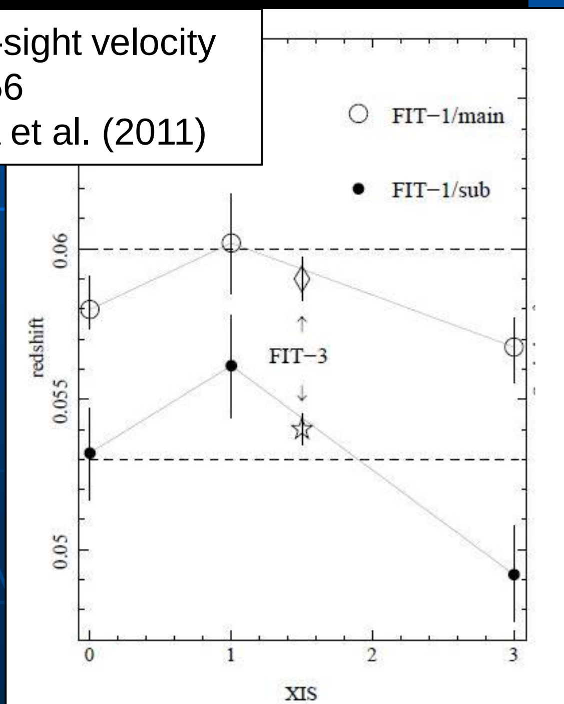

Line-of-sight velocity of A2256
Tamura et al. (2011)

- Well-known local (z=0.0581) merging cluster
- Two components in member galaxy l.o.s. velocity distribution（Berrington et al. 2002）
- Two distinct peaks in X-ray image(Briel et al. 1991, etc)
- Only one example of direct detection of ICM internal motions(～1500km/s) (Tamura et al. 2011)
- Radio halo and relics (Clarke&Ensslin 2006, etc)

Observations

Table 1. Details of the VLA & JVLA observations of Abell 2256.

Frequency* (MHz)	Bandwidth* (MHz)	Config.*	Date	Time* (h)	Project*
1369/1417	25/25	D	1999-Apr-28	5.9, 5.9	AC0522
1513/1703	12.5/25	D	1999-Apr-29	3.5, 5.5	
1369/1417	25/25	C	2000-May-29	2.5, 2.5	AC0545
1513/1703	12.5/12.5	C	2000-May-29	3.6, 3.6	
1369/1417	25/25	C	2000-Jun-18	2.5, 2.5	
1513/1703	12.5/25	C	2000-Jun-18	4.1, 3.5	
16 windows†	128	C	2013-Aug-25	1.2	13A-131
S-band			2013-Aug-26	1.2	
			2013-Aug-29	1.2	
16 windows‡	128	C	2013-Aug-18	1.3	13A-131
X-band			2013-Aug-19	1.3	

* Column 1: observing frequency; Column 2: observing bandwidth; Column 3: array configuration; Column 4: dates of observation; Column 5: time on source; Column 6: NRAO project code.

† 2051/2179/2307/2435/2563/2691/2819/2947/3051/3179/3307/3435/3563/3691/3819/3947.

‡ 8051/8179/8307/8435/8563/8691/8819/8947/9051/9179/9307/9435/9563/9691/9819/9947.

- multi-band polarimetric observations, to explore the magnetic field trough depolarization and rotation measure
- S-band (2051-3947MHz)
- X-band (8051-9947MHz)

August 2013, JVLA

- L-band (1369-1703MHz) archive data of VLA

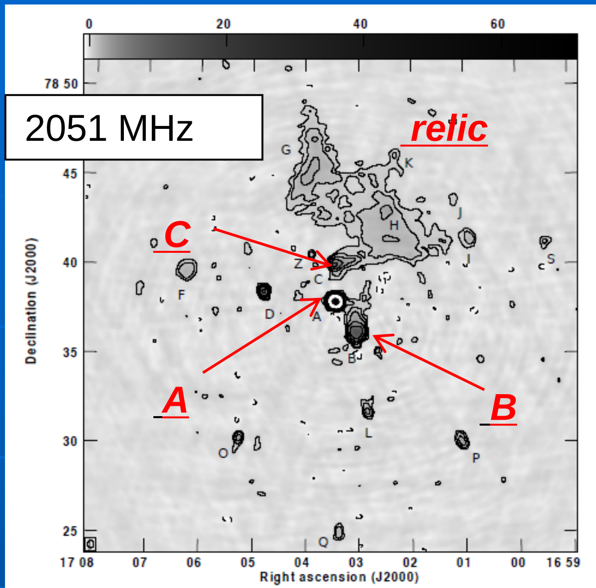

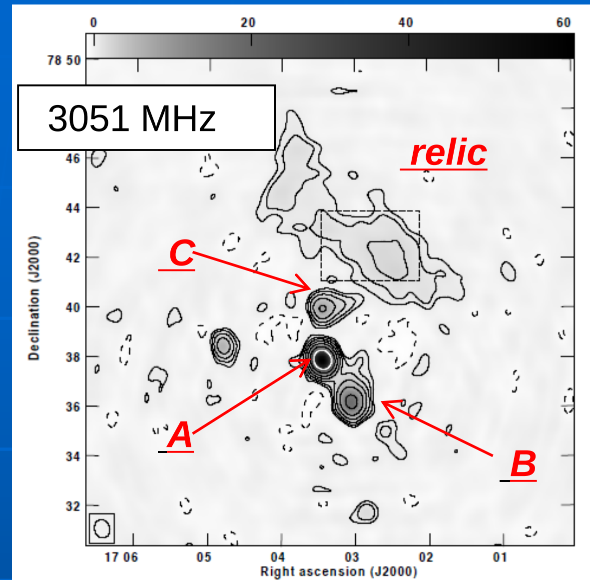

Radio images

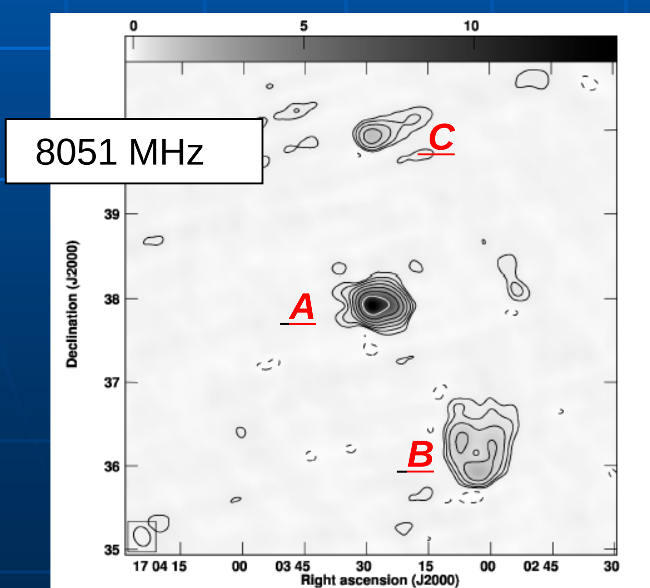

- relic, source A--Z (point sources such as radio galaxies)
- In S-band, polarized components are detected from relic, A, and B
- In X-band, polarized components are detected only from source A（relic is out of FOV）。

Fractioal Polarization Spectra of the Relic

$$\mathrm{FPOL} = \frac{\sqrt{\mathrm{Q}^2 + \mathrm{U}^2}}{\mathrm{I}}.$$

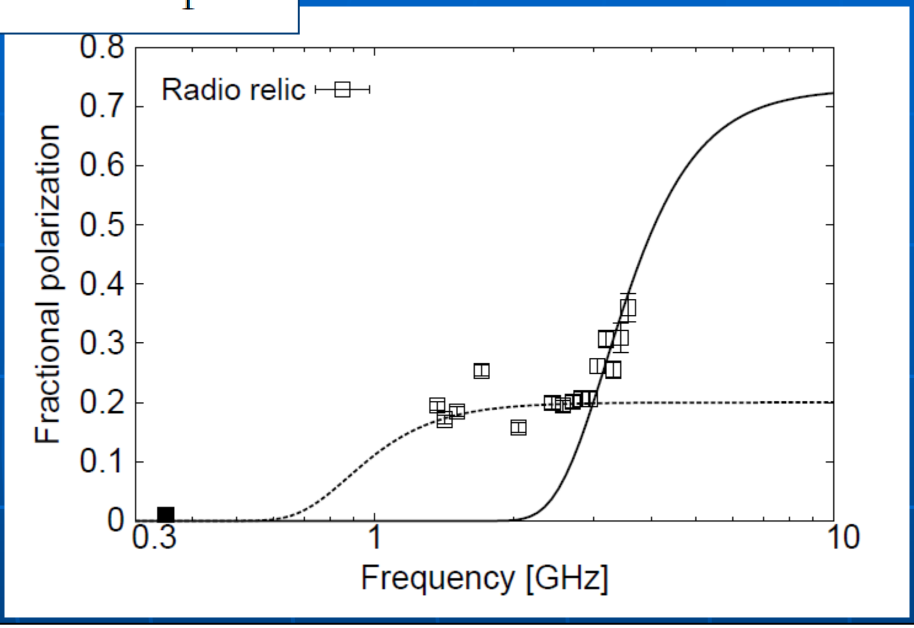

Fractional polarization spectra of the radio relic
FPOL=p exp(-S), (Burn's law)
p: intrinsic FPOL, $S = 2\sigma_{RM}^2 \lambda^4$

- Fractional polarization specta have two distinct strucures（～0.8GHz, ～3GHz）
- Random magnetic field between the relic and us cause depolarization.
- However, a simple external Faraday dispersion (EFD) model cannot reproduce this kind of spectral shape.
- There might be two depolarization components ？？？

simple EFD

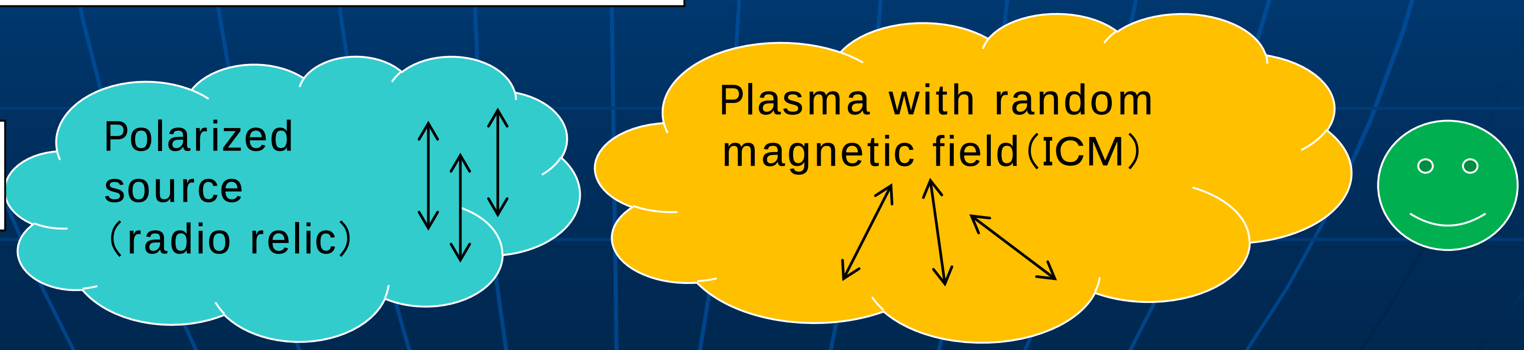

Depolarization toward the Radio Relic

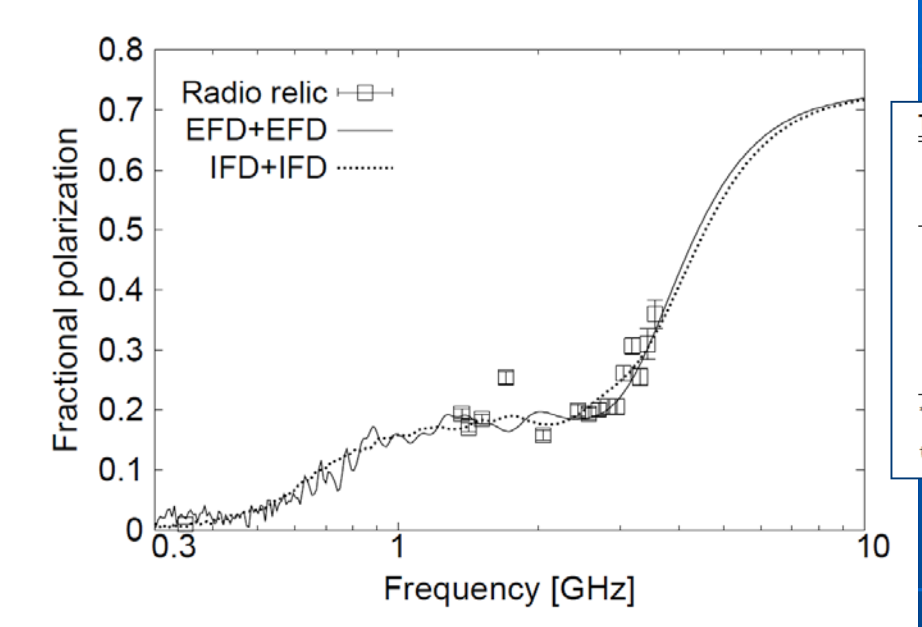

Table 4. Parameters for the Depolarization Models.

Model	Component	B	n_e	Δl	$N_X \times N_Y$	N_Z	Intensity	$\sigma_{\rm RM}$
		[μG]	[10^{-3} cm^{-3}]	[kpc]	[kpc $\times$ kpc]	[kpc]		[rad m^{-2}]
EFD+EFD	foreside	0.3	3.0	1*	50×50 *	500	1	6.3
	backside	5	10.0			25 †	5	128.5
IFD+IFD	foreside	0.5	1.0	1 *	50×50 *	500	1	5.2
	backside	10	10.0			25 †	4.5	228.3

* We assume 50×50 kpc since the beam size of $47''$ corresponds to $\sim$52 kpc.

† We assume that the thickness of the radio relic is 25 kpc (Owen et al. 2014).

EFD+EFD

Polarized sources (relic???)

Depolarization component (relic???)

Polarized source (relic???)

Depolarization component (ICM or Galactic)

IFD+IFD

Polalaized source and Depolarization component (relic???)

Polarized source and Depolarization component (ICM or Galactic)

Rotation Measure

RM map

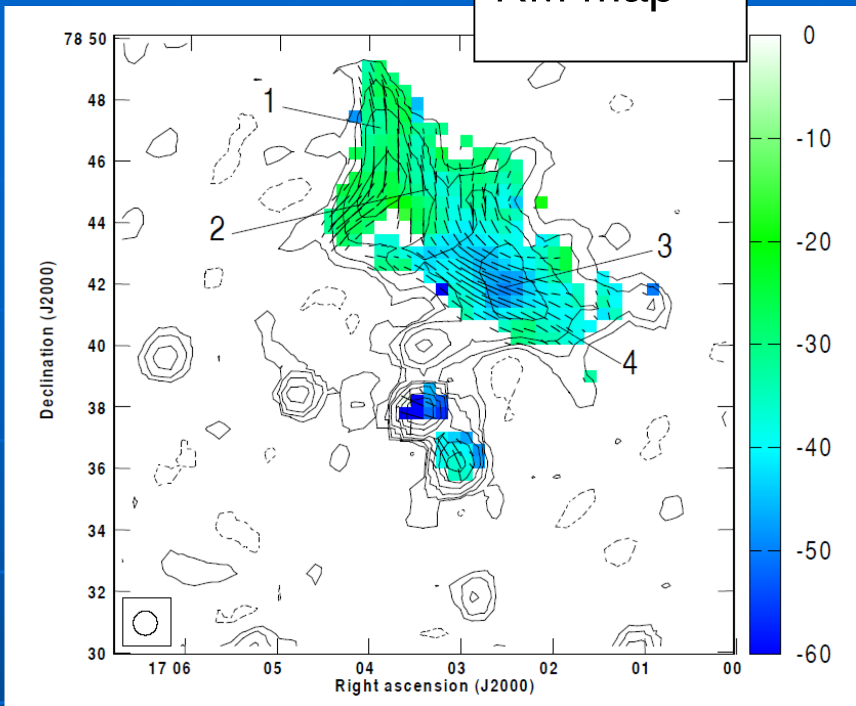

Table 3. The average and standard deviation of RM.

Target	$\langle \mathrm{RM} \rangle^*$ rad m^{-2}	$\sigma_{\mathrm{RM}}{}^*$ rad m^{-2}	reference
Relic	-44	7	Clarke & Ensslin (2006)
Relic	-34.5	6.2	this work
Source A	-24.9	65.5	this work
Source B	-34.1	10.5	this work

* $\langle \mathrm{RM} \rangle$ and σ_{RM} are the average and standard deviation of RM, respectively.

ϕ vs λ^2

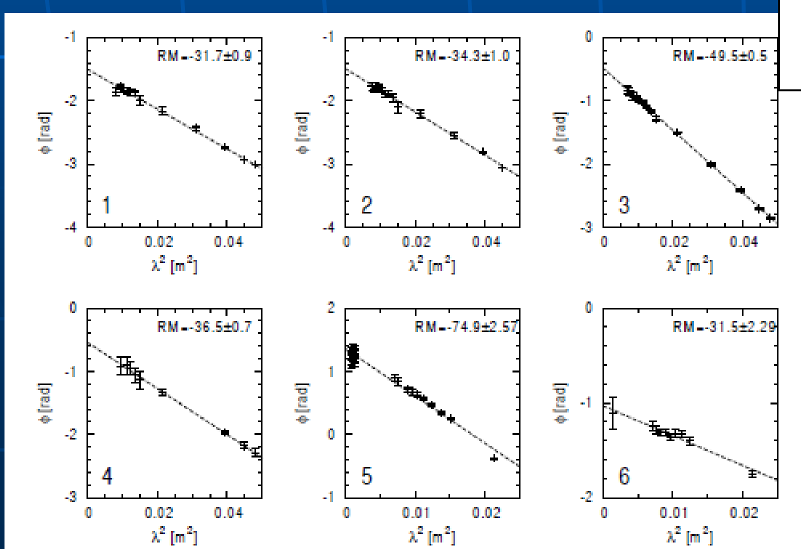

- <RM>～ -30 rad/m^2

  This value is consistent with a contribution from the Galactic component
- In relic, σ_{RM} is significantly smaller than that of sources A.

  -→The relic is located in the nearer side of the observer in the cluster

Merger geometry and relic formation scenario

Early phase scenario

Late phase scenario

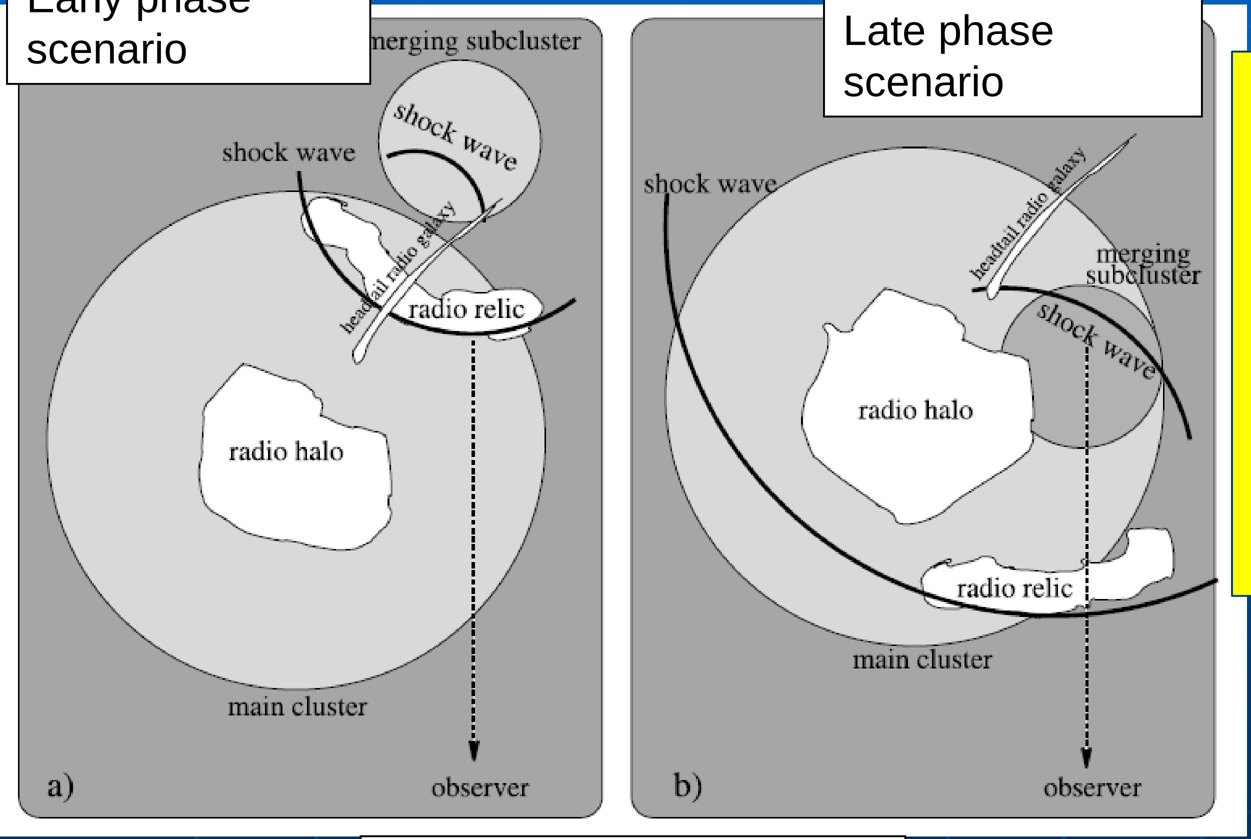

Clarke&Ensslin(2006)

Considering small σ_{RM} value, relic is likely located nearer side of us in the cluster.

This fact favors “Late phase scenario”.

Summary

- S- and X-band polarimetric observations were made with JVLA for well-known merging cluster Abell 2256 with radio relics.
- Fractional polarization spectra of the relic have characteristic structures, which can be reproduced assuming that two depolarization components are located along the line-of-sight.
- Considering small value of σ_{RM}, it is suggested that the radio relic is located at the nearer side of us. This indicates that a late phase scenario of merger is preferable.
- Ozawa et al. (2015) PASJ, 67, 110

Magnetic Fields toward Source A and B

l: coherent length of the field

L: length of the object

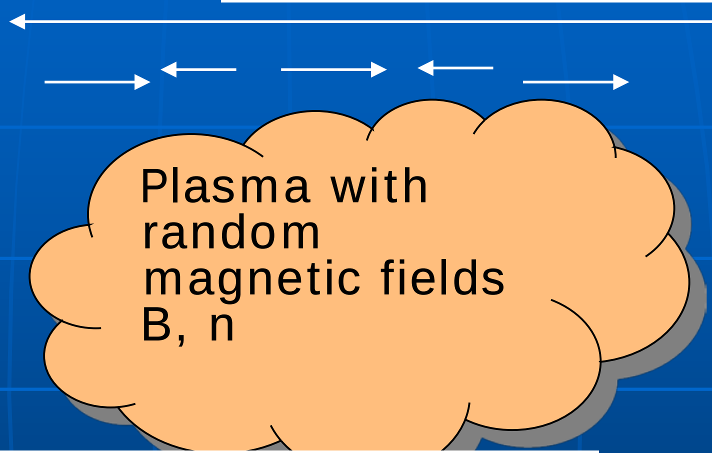

$\Delta\theta$ behaves like random walk processes.

$\Delta\theta \sim \lambda^2 n B_{//} (lL)^{0.5}$

$$\sigma_{\rm RM} = \frac{K B n_0 r_c^{1/2} \Lambda_B^{1/2}}{(1 + r^2/r_c^2)^{(6\beta-1)/4}} \sqrt{\frac{\Gamma(3\beta - 0.5)}{\Gamma(3\beta)}},$$

Table 6. Parameters for magnetic field strengths.

Source	X-ray morphology	K	$\sigma_{\rm RM}$ [rad m^{-2}]	n_0‡ [10^{-3} cm^{-3}]	r** [kpc]	r_c‡ [kpc]	β‡	Λ_B [kpc]	B [μG]
Abell 2256 A	Irregular	441	65.5	2.6	7.2	587	0.914	20–5	0.63–1.26
Abell 2256 B	Irregular	441	10.5	2.6	133.7	587	0.914	20–5	0.11–0.21

Faraday Tomography for the relic

QU-fit for relic

Black lines: two components model

Grey lines: one component model

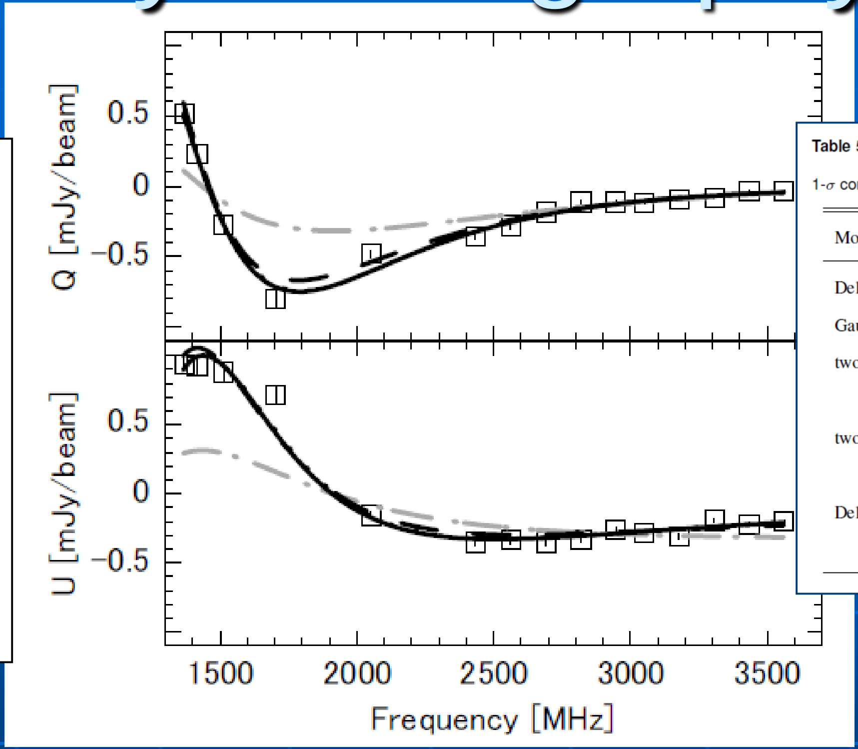

Table 5. The reduced chi-square (RCS), the Bayesian information criterion (BIC), and best-fit values and 1-σ confidence regions for model parameters in the QU-fit.

Model	RCS	BIC	ϕ	Amp.	χ_0	Width
Delta function	38.8	1173.1	$-41.29^{0.713}_{-0.688}$	$0.32^{0.005}_{-0.005}$	$-0.56^{0.009}_{-0.009}$	
Gaussian	38.8	1176.5	$-41.28^{0.704}_{-0.710}$	$0.32^{0.005}_{-0.005}$	$-0.56^{0.009}_{-0.009}$	$0.00^{0.675}_{0.008}$
two Deltas	5.0	170.0	$-46.71^{0.972}_{-0.971}$	$3.86^{0.207}_{-0.049}$	$0.35^{0.051}_{-0.040}$	
			$-43.74^{0.914}_{-1.111}$	$3.92^{0.107}_{-0.054}$	$-1.22^{0.050}_{-0.039}$	
two Gaussians	3.8	142.0	$-40.87^{3.446}_{-0.722}$	$6.14^{0.106}_{-0.231}$	$0.37^{0.009}_{-0.066}$	$11.99^{3.078}_{-0.959}$
			$-38.25^{3.326}_{-0.805}$	$6.20^{0.090}_{-0.242}$	$-1.20^{0.008}_{-0.064}$	$10.43^{1.851}_{-1.034}$
Delta + Ganssian	3.9	139.6	$-57.53^{1.945}_{-0.528}$	$0.70^{0.357}_{-0.233}$	$0.33^{0.020}_{-0.087}$	
			$-34.43^{3.937}_{-7.701}$	$0.74^{0.343}_{-0.236}$	$-1.26^{0.041}_{-0.154}$	$10.01^{6.586}_{-1.297}$

- Farady tolmography（QU-fit、Ideguchi et al. 2014）for the relic
- Two polaried sources at different Faraday depth are necessary.
- Note: In QU-fit, information about polarization angles is also used. However, we can locate polarized sources only in the Faraday depth space (not real space).

Intracluster Magnetic Field

- There is random magnetic field in the intracluster space, whose typical strength is ~ μG.
  - Shyncrotron radio halos/relics
  - Faraday rotation measure
- $P_B \sim 0.01 P_{th}$ not important?
  - suppression of fluid instabilities
  - suppression of heat conduction
  - Particle acceleration (magnetic turbulence, shock)
- Not only field strength, but also field structures are important.